THE ROLE OF PASSIVE FILM GROWTH KINETICS AND PROPERTIES IN STRESS CORROSION AND CREVICE CORROSION SUSCEPTIBILITY

NATIONAL BUREAU OF STANDARDS
WASHINGTON, D. C.

NOVEMBER 1976

026079

NBSIR 76-1170

The Role of Passive Film Growth Kinetics and Properties in Stress Corrosion and Crevice Corrosion Susceptibility

J. Kruger and J. R. Ambrose

Corrosion and Electrodeposition Section
Metallurgy Division
Institute for Materials Research
National Bureau of Standards
Washington, D. C. 20234

D D C
JAN 24 1977
C

NBSIR 76-1170

THE ROLE OF PASSIVE FILM GROWTH KINETICS AND PROPERTIES IN STRESS CORROSION AND CREVICE CORROSION SUSCEPTIBILITY

J. Kruger and J. R. Ambrose

Corrosion and Electrodeposition Section
Metallurgy Division
Institute for Materials Research
National Bureau of Standards
Washington, D. C. 20234

November 1976

Technical Summary Report Number 7

DISTRIBUTION OF THIS DOCUMENT IS UNLIMITED

[To be included in the Proceedings of Symposium on Inhibitors for Localized Corrosion, NACE National Meeting, San Francisco, March 1977.]

THE ROLE OF MOLYBDENUM AS AN INHIBITOR OF LOCALIZED CORROSION

ON IRON IN CHLORIDE SOLUTIONS

J. R. Ambrose
Institute for Materials Research
National Bureau of Standards
Washington, D. C. 20234

ABSTRACT

A series of Fe-xMo alloys, where x ranged from 0 to 6 weight percent, were used to determine the effect of molybdenum concentration on the repassivation kinetics of iron within a crevice. Results show that concentrations of molybdenum greater than 5 weight percent are effective in increasing the repassivation rate. Resistance of these alloys to crevice corrosion attack appears to result from the role of molybdenum in the formation of a protective salt film following breakdown of passivity within a crevice.

Introduction

The term "Inhibitor for Localized Corrosion" has come to be associated with some additive which, when introduced into an environment, improves the resistance of a particular metal to pitting, crevice, or stress corrosion cracking. However, recent studies have shown that certain alloying elements, molybdenum as a case in point, behave in a fashion similar to what has come to be expected for inhibitors added directly to the solution. In other words, the mechanism by which the localized corrosion processes is inhibited is the same whether the element is alloyed into the metal, or whether its anodic dissolution product is added to the solution. Reports of such behavior have been published for molybdenum, chromium, vanadium, silicon and several other less common alloying elements (1-7). As a caterpillar can protect itself when it generates its cacoon, more efficient protection of an alloy may be likely when the alloy generates its own inhibitors.

A study by Kodama and Ambrose (1) showed that the molybdate ion, which is the anodic dissolution product of molybdenum, would inhibit propagation of pits but not their initiation. The explanation of this effect was based on the observation that these repassivated pits contained measurable amounts of the element molybdenum possibly in the form of $FeMoO_4$. What was not readily available from these experiments was a detailed knowledge of how these pits repassivated; if a salt film was involved, how fast did it grow? To meet the need to examine the changes occurring at the metal surface, a technique was developed (8) for ellipsometric measurements of optical changes inside the crevice created by placing a quartz plate adjacent to a reflective metal surface. Using this technique, the effect of introducing a crevice on film growth and dissolution kinetics on iro could be measured and related to electro-chemical changes.

This paper is concerned mainly with the role molybdenum plays in iron repassivation kinetics and hence how repassivation rates could be expected to control susceptibility to localized corrosion processes. It is becoming increasingly recognized that repassivation is one of the major basic processes affecting localized corrosion (9). To measure repassivation kinetics in a crevice presents certain difficulties. For example, cathodic reduction of surface film on iron within a crevice is impossible in the presence of a reducible species such as $MoO_4^=$. Addition of the ion just before repassivation is measured is also a difficult procedure. Therefore, a series of binary Fe-Mo alloys was prepared with the intention of comparing results from this study with those obtained when molybdate was added directly to the solution. The work described here involves repassivation of iron-molybdenum alloys in sodium borate-boric acid solutions to which sodium chloride solution was added. These studies, in addition to providing some answers to the question of role of molybdenum as an inhibitor, also point to future work necessary to evaluate inhibitor performance.

-2-

Experimental

Binary iron-molybdenum alloys of composition Fe-xMo, where x ranged from 0 to 6 weight percent, were prepared from high purity materials (see Tables I and II). The iron had previously been annealed in hydrogen to remove reducible species. The alloys were homogenized for 72 hours at 1000 °C and under a vacuum of not less than 5×10^{-7} torr, then furnace cooled. Cylindrical specimens were machined from the castings using an electrical discharge spark erosion process and then mounted in an epoxy resin. The mounted specimens were then drilled and tapped for electrode assembly. A short section of glass tubing was cemented with epoxy resin into a hole drilled completely through the electrode and was connected via a flexible piece of surgical tubing to the salt bridge of the reference electrode assembly. This particular arrangement permits measurement of electrode potentials within a crevice (Fig. 1). The remainder of the crevice electrode assembly (Fig. 2) was the same as that used in previous studies (10).

Specimens were polished using silicon carbide metallographic papers, then polished on a wheel using 6 μm and finally 1 μm diamond pastes. Following polishing, specimens were ultrasonically cleaned with ethyl alcohol, rinsed with spectro-grade methanol, dried in air, then mounted in the teflon retaining ring. The entire crevice electrode assembly, with the quartz disk in place (Fig. 3) was stored in a vacuum desiccator until ready for exposure to the solution.

All experiments were performed using solutions prepared from reagent grade chemicals and distilled water (7×10^{-7} ohm^{-1} cm^{-1}). A buffer solution containing 9.3 g H_3BO_3 and 14.3 g $Na_2B_4O_7 \cdot 10$ H_2O per liter (pH 8.4) was used as a stock solution. Solutions containing chloride ion were prepared by adding an aliquot of 1.0 N NaCl solution to the stock solution. The chloride ion concentration used in these studies was 5×10^{-3} N in all cases.

Just prior to positioning the crevice electrode assembly in place on the ellipsometer, the crevice thickness was set by spacing the quartz disk 0.25 mm from the metal surface using a teflon shim. After connection to a potentiostat and transient detection equipment, the crevice electrode was flushed with fresh solution through the salt bridge. Surface air-formed films were reduced electrochemically at -758 mV SHE with the potentiostat. After a period of approximately ten minutes, when the cathodic current level had stabilized, ellipsometer readings and calibrations were made. The potential was then stepped to +242 mV SHE; current and charge transients were recorded on an oscilloscope with extended time transients being measured on a strip chart recorder. A similar procedure was followed in those experiments where no crevice was present.

-3-

Table I. Iron Composition

Heat No.	Impurity Element	Content (weight percent)	Impurity Element	Content (weight percent)
C80022-1	C	.006	Co	.003
	Mn	.001	Cu	.001
	P	.003	Al	.01
	S	.007	Sn	.001
	Si	.008	Pb	.0006
	Ni	.03	O_2	.026
	Cr	.01	H_2	.00006
	V	.004	N_2	.0004
	W	.01		
	Mo	.001		

Table II. <u>Molybdenum Composition</u>

Impurity Element	Content (wt.ppm)	Impurity Element	Content (wt.ppm)	Impurity Element	Content (wt.ppm)
O	< 10.0	Ca	0.2	Nb	3.0
C	40.0	Sc	< 0.4	Ag	< 2.0
F	< 6.0	V	0.5	Cd	<20.0
Mg	< 2.0	Cr	0.02	In	< 1.0
Al	0.1	Mn	2.0	Sn	< 1.0
Si	2.0	Fe	0.1	Te	<15.0
P	< 0.1	Co	0.04	Ta	< 6.0
S	< 0.6	Ni	< 10.0	W	60.0
Cl	0.4	Cu	0.04	Au	< 6.0
K	0.2	Zr	< 10.0	Pb	< 0.4

Others <0.1ppm

In each case, simultaneous measurement of decrease in ellipsometer light intensity (proportional to film thickness) was made using an off-null technique (11). After each experiment, the electrode was disassembled, the specimen repolished, solutions changed, and the entire process repeated. Results are based upon an average of two consecutive runs.

Results

In 5×10^{-3} N buffered chloride solutions, repassivation at 242 mV SHE following cathodic film reduction at -758 mV SHE took place in two distinct stages. During Stage I the anodic current generated as a result of the potential step was found to decrease at a rate proportional to the concentration of molybdenum in the alloy when the alloy was exposed within a crevice. Current decayed until a time interval proportional to the molybdenum concentration in the alloy had elapsed. At this point in time, referred to as t_{ss}, the current ceased to decay, and what will be called Stage II began. During Stage II, metal dissolved at a fixed rate inversely proportional to the concentration of molybdenum in the alloy.

In Fig. 4 the anodic charge consumed during the repassivation for three of the materials used in this study is plotted as a function of the square root of time; no crevice was present. During Stage I, where the data points fall along straight lines, current is decreasing. Steady state current levels are indicated by deviations of data points from the straight lines. The time at which these deviations appear is labeled t_{ss} in the figure. The effect of increased molybdenum content in the alloy is evident from the observation that the decrease in the rate of consumption of charge goes from 10^{-1} coulombs $sec^{-1/2}$ for Fe-1 Mo to 7×10^{-2} coulombs $sec^{-1/2}$ for Fe-3 Mo to $3.1 \times 10_s^{-2}$ coulombs $sec^{-1/2}$ for Fe-5 Mo. Moreover, t_{ss} increases from approximately 200 milliseconds to over 1000 milliseconds as the molybdenum concentration in the alloy is increased from 1 to 5 weight percent. Finally, the Stage II constant current level decreases from 365 to 7.3 milliamperes as the molybdenum content increases from 1 to 5%. Interestingly enough, for the same Stages I and II, values of current intermediate between those for Fe-3 Mo and Fe-5 Mo were found for pure iron (5.3×10^{-2} coulomb $sec^{-1/2}$ and 11.8 milliamperes, respectively). These results are tabulated in Table III.

For alloys exposed to the crevice, somewhat more irregular behavior was measured. Within a crevice, no repassivation of pure iron occurred since the current did not decay from its initial peak value. The effect of molybdenum addition is shown in Table IV. Although pronounced decreases in current level are evident as the Mo concentration is increased to 5 weight percent, an anomolous behavior is observed for the Fe-3 Mo alloy. Here, current levels are somewhat higher than the values measured for the Fe-1 Mo alloy.

-6-

Table III. Non-Crevice Repassivation Kinetics

% Mo	Stage I Dissolution Rate ($\times 10^3$), coulomb-sec$^{-1/2}$	Stage II Dissolution Rate mA
0	53	11.8
1	100	36.5
3	70	24.6
5	31	7.3

Table IV. Crevice Repassivation Kinetics

% Mo	Stage I Dissolution Rate ($\times 10^3$) coulomb-sec$^{-1/2}$	Stage II Dissolution Rate, mA
0	--*	83
1	115	7.6
3	240	15.1
5	72	6.3

* no current decay from peak value observed.

One consistent observation could be made, however. Introduction of the crevice delayed the onset of Stage II in each alloy studied. In other words, the current would continue to decrease for longer time intervals when the crevice was in place than when it was not present. This leads, of course, to lower steady state current values (Stage II) for a given alloy composition inside a crevice as compared to the t_{ss} found with no crevice. Finally, as shown in Fig. 5, current levels, hence rate of charge consumption for the Fe-5 Mo alloy during Stage I, were higher inside the crevice than outside. The phenomonology was the same for the other alloys studied.

Ellipsometer measurements were made simultaneously with the electro-chemical ones. The off-null technique was used in which optical changes which occur at the metal surface give rise to changes in the photocurrent intensity measured during the repassivation transient. Results for three alloys, when not exposed to a crevice, are shown in Fig. 6. Here, changes in intensity, which are proportional to ΔP (change in polarizer angle) and also to film thickness, are plotted against the log of the square root of time. Although rates of change of surface optical properties are about the same, the relative magnitude of ΔP is less for the higher molybdenum-containing alloy.

Similar measurements for the material exposed within a crevice were not as successful. Due to the electrode configuration in this particular cell, the position of the counter electrode with respect to the specimen resulted in most of the cell current being consumed at an area on the working electrode surface which was closest to the auxiliary electrode. This particular area happened to be out of view by the ellipsometer. A new electrode design, which incorporates the counter electrode into the specimen as a ring around the working electrode (Fig. 7), promises to allow better current distribution to the working electrode and more meaningful ellipsometer measurements.

Discussion

1.   Role of mass transport in repassivation kinetics

The study by Kodama and Ambrose (1), in which additions of $MoO_4^=$ to chloride containing solutions appeared to affect the propagation stage of pitting, showed the effect of increased concentration of the molybdate ion (Fig. 8). Repassivation of these pits was attributed to the formation of a stable salt film which restricted metal dissolution. Similar results, which also may be explained by the formation of a molybdate containing salt film, were obtained in this study.

Stage II repassivation kinetics as described here correspond to the plateau areas in Fig. 8 where pits already initiated are beginning to cease to propagate. By using a crevice, however, it is possible to magnify the area of localized corrosion to such an extent that more careful examination of the influence of molybdenum (or its anodic dissolution product, $MoO_4^=$) is possible. By comparing what happens when a crevice is present to what happens when it is absent makes it evident that, for molybdenum to affect the repassivation kinetics of the material to which it is alloyed, it must be introduced into the environment under conditions of severe mass transport limitations. We can see, for instance, that when repassivation with and without a crevice are compared, although the metal dissolution rate for unalloyed iron is some 7 times higher during Stage II crevice repassivation (Tables III and IV), the effect of alloyed molybdenum is to decrease the dissolution rate during Stage II over that measured without a crevice. This increase in repassivation efficacy occurred even when current levels were significantly higher during Stage I repassivation (Fig. 5). What this suggests is that unless the anolyte becomes very concentrated with the molybdate ion, the dissolution rate of any salt film containing this ion will be of such magnitude to preclude its stable existence for long enough periods of time to afford protection. This suggestion also explains why, in the previous study (1), molybdenum was only detected within those pits which had initiated, but which subsequently had failed to propagate. Restricted geometries of these pits provided the limited mass transport conditions necessary to build up a high concentration of molybdate ion, to allow formation of a stable salt film, and then to prevent dilution of the molybdate solution in these newly passivated pits by diffusion of the ion into the bulk solution. Consistent with

-8-

the idea of formation of a salt film is the experimental evidence that the degree of repassivation is related to the concentration of the molybdate ion in solution during the pitting of iron (1) and to the magnitude of anodic dissolution found during crevice corrosion in this study. Several critical experiments remain to be done to test this suggestion whether an insoluble salt film may be forming. Accurate anolyte solution analysis with respect to iron and molybdate ions is needed to establish concentration profiles within the crevice volume. Secondly, surface profile analysis of the exposed metal must show that molybdenum can indeed be enriched under those conditions of limited solution mass transport. The results of these particular experiments would go a long way to explain the results of researchers (12) who, using Auger Electron Spectroscopy techniques, fail to observe surface molybdenum enrichment following anodic dissolution in ferritic stainless steels.

2.   What affects salt film formation?

Accepting for the moment the idea that formation of salt films of the sort suggested by Kodama and Ambrose is possible, several questions remain to be answered:

a. What parameters determine the effectiveness of a particular material in enhancing repassivation behavior? Are they related to initial rate of formation, overall uniform thickness, stability under a wide range of solution pH, potential, chloride ion concentration?

b. What is so special about molybdenum? Can the properties of the alloyed metal and its dissolution products be used to predict performance of other suggested inhibitors - whether they be in the form of an alloy or as an additive to the environment?

Some answers come from examination of data obtained during Stage I repassivation. If anodic current decay can be related to thickening of a protective surface film, then it may be supposed that so long as the film grows, current will continue to decrease. From Table III it can be seen that the rate of current decay is related to % Mo in the alloy. In Fig. 4 it is shown that the time during which current continues to decay is also proportional to the molybdenum concentration in the alloy. Thus, for the case where no crevice is present, it seems clear that molybdenum can contribute to improved repassivation behavior by stimulating formation of a thicker, more protective surface film. However, we should temper our conclusions by examining what the ellipsometer measurements show with regard to what is happening on the metal surface. From Fig. 6, it can be seen that these measurements do not show this to be true - in fact the inverse relationship is demonstrated. Such results are not surprising, however, when one remembers that $k\Delta P$ is proportional not only to film thickness but also to degree of surface roughening (pitting) and to accumulations of non-protective corrosion

-9-

product deposits. What Fig. 6 does show then, is that deterioration of the surface is restricted as the molybdenum concentration is increased. One other point should be kept in mind. The requirement of solution mass transport limitation already discussed is met only within the pits initiated on the surface, or in the crevice used in this study. No ellipsometer currently available can measure the optical changes that occur within these pits.

Current densities measured during the course of this study were found to range from 1 - 100 mA/cm^2. When we distribute this current in proportion to the composition of the alloy, one can get an idea of the rate of build-up of molybdate ion as approximately 10^{-3} equivalents liter^{-1} sec^{-1}. After about 1 second, the concentration of molybdate in this particular crevice volume would be 10^{-3} N, or roughly equal to the minimum concentration of $MoO_4^=$ necessary to inhibit pit propagation on iron in chloride solutions of 10^{-2} N (1). It should be remembered, however, that sufficient molybdate must be available to produce a salt film of critical thickness before the solution has deteriorated too far. Once pH and chloride ion concentrations have reached levels where the salt film remains unstable, propagation of pits or crevice attack cannot be stopped. Hence, the fact that low molybdenum composition alloys do not improve corrosion resistance of pure iron, no matter how long one waits to build up the concentration of $MoO_4^=$ ion in the restricted volume of solution.

3. Is molybdenum always beneficial?

A word of caution is necessary before completely accepting the existence of effects of molybdenum in iron. In Table III it can be seen that the addition of 1% molybdenum to iron actually results in a decrease in the Stage I repassivation rate as well as in increase in the steady state corrosion during Stage II. In fact, no real improvement over the performance of pure iron is noticed until the molybdenum concentration in the alloy reaches 5%. This effect is magnified when a crevice is present (see Table IV) since we are obviously dealing with a much larger volume of solution in which mass transport is limited. This observation emphasizes the concerns of question 1. It is intuitive that additions of molybdenum should change the properties of a surface film. But which way? It stands to reason that if a film on iron is protective enough under a given set of conditions, then it is useless to try to affect the properties of that film so long as those conditions prevail. But when conditions are altered such that the film becomes non-protective, as it is during pitting or crevice corrosion attack, it is then that an improvement in the protection properties of a surface film is required. Thus, during early stages of repassivation of iron when solution pH and composition are such that if insufficient concentrations of molybdate are available, the film formed will not be as protective as if no molybdenum were present at all. It also appears, all other things being equal, that a critical concentration of molybdenum, whether present in the metal or in solution, is necessary to provide a more or less uniform

-10-

film of a critical thickness. It appears that the minimum molybdenum concentration for these Fe-Mo binary alloys is around 5%. Introduction of other alloy constituents would probably have a pronounced effect on the value (10). This study showed that increased concentrations of chromium improved upon the effect of addition of molybdenum.

4. What remains to be done?

It is hoped that verification of the presence of the salt film and its thickness dependence on molybdenum concentration in the alloy during crevice repassivation will come from use of the new specimen design (Fig. 7). These results coupled with solution microanalyses, and surface profile analysis with ESCA or Auger spectroscopy will go a long way towards answering a great many of the questions which have arisen from an interpretation of the results obtained in this work.

Conclusions

1. Additions of less than 5% molybdenum are detrimental to the repassivation kinetics of iron with a crevice present or not.

2. Repassivation of these Fe-Mo binary alloys takes place in two stages - Stage I, where current decreases are measured, and Stage II, where a steady state current level is observed. Stage I corresponds to salt film growth, Stage II to constant salt film thickness.

3. Introduction of a crevice results in an increase in the metal dissolution rates for a given alloy composition during Stage I repassivation. However, Stage II steady state corrosion rates are decreased within a crevice as the molybdenum concentration in the alloy is increased.

4. Results are interpreted on the basis of formation of a protective film during repassivation. A critical thickness of film formed within a critical time interval will determine whether the particular localized corrosion process will propagate or not.

5. Solution composition analysis, surface profile analysis and improved ellipsometer measurement techniques should resolve many of the interpretations presented as a result of repassivation kinetics measurements of these iron-molybdenum binary alloys.
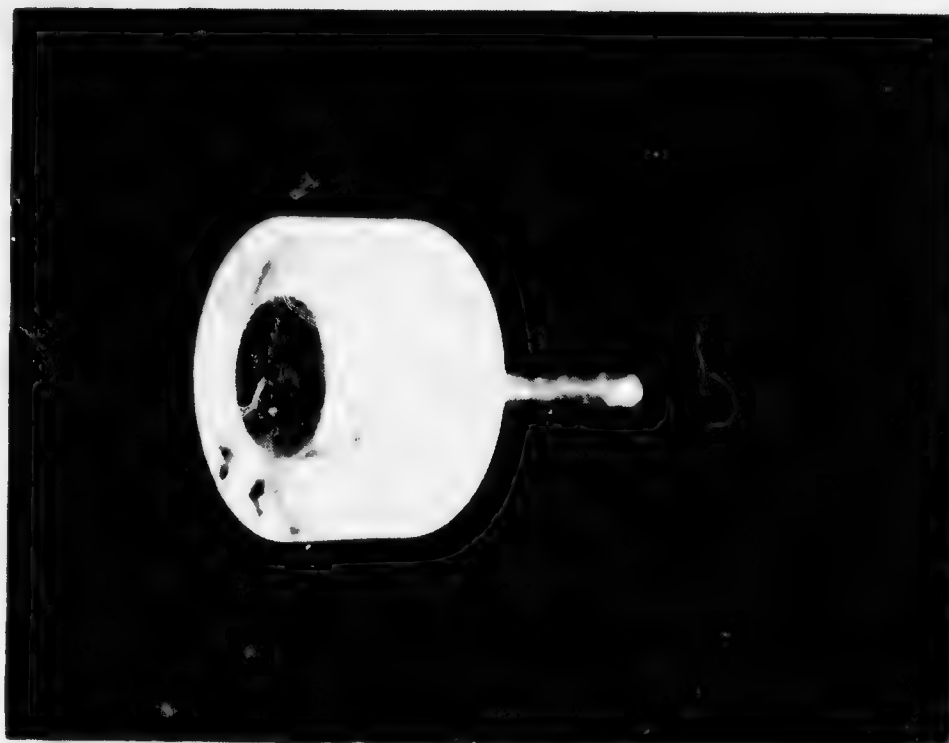
Fig. 1. Fe-3Mo alloy mounted in epoxy resin. The reference electrode
salt bridge can be attached to the glass tubing which
protrudes from the rear of the electrode.

-12-

Fig. 2. Components of the crevice electrode. Shown from top right
to bottom left are the working electrode attached to a
plexiglass support, a stainless steel rod for electrical
connection to the specimen, the quartz disk and teflon
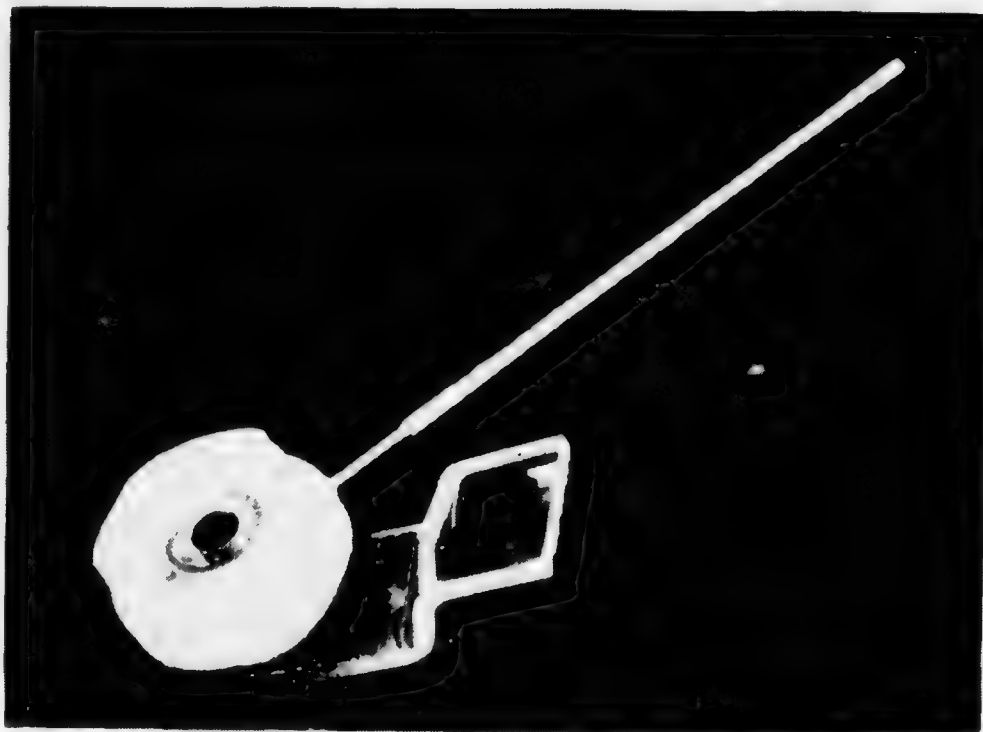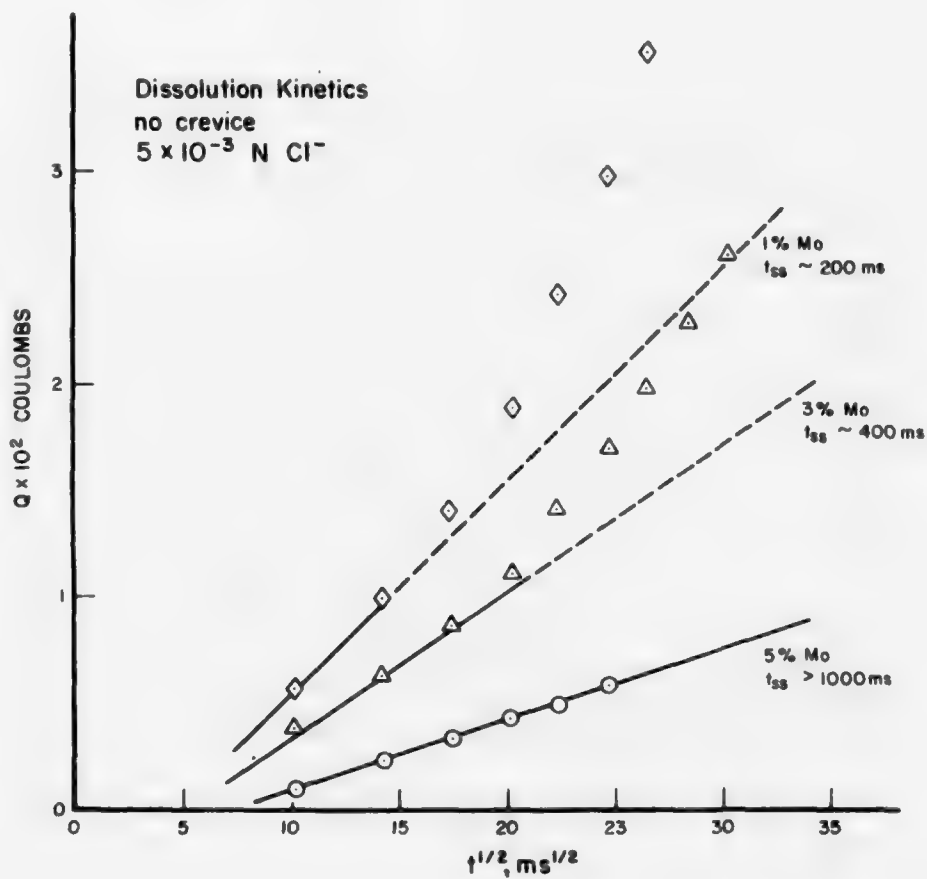adapter used for making the crevice.

Fig. 3. Assembled crevice electrode system.

-14-

Fig. 4. Plot of charge consumed, Q, versus square root of time, ms$^{1/2}$ for Fe-xMo (x=1,2,3,) during repassivation at 242 mV SHE in the sodium borate-boric acid buffer; chloride ion concentration = 5 x 10^{-3} N.

-15-

Fig. 5. Comparison of dissolution kinetics of Fe-5Mo within and without a crevice. Plotted are changes in consumed charge, Q, versus square root of time, $ms^{1/2}$, Repassivation occurs at 242 mV SHE in the sodium borate-boric acid buffer; chloride ion concentration = 5×10^{-3} N.

-16-

Ellipsometer Changes During Repassivation

Fig. 6. Plot of ellipsometer variation, k∆P versus logarithm square root of time, 1/2 $\log_{10} t$, in ms, for Fe-xMo (x = 1,2,3,) with no crevice in place. Repassivation occurs at 242 mV SHE in the sodium borate-boric acid buffer; chloride ion concentration = 5 x 10^{-3} N.
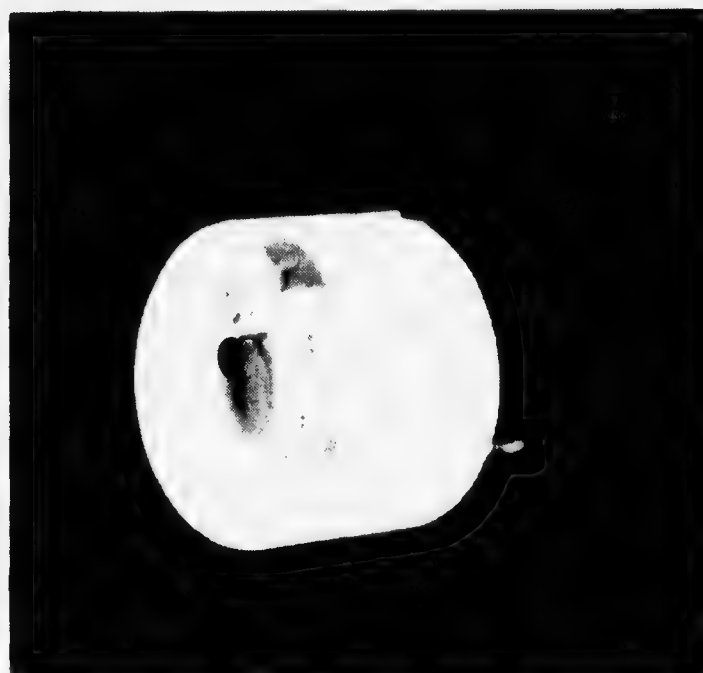
-17-

Fig. 7. Fe-3Mo alloy with encircling platinum electrode mounted in epoxy resin.
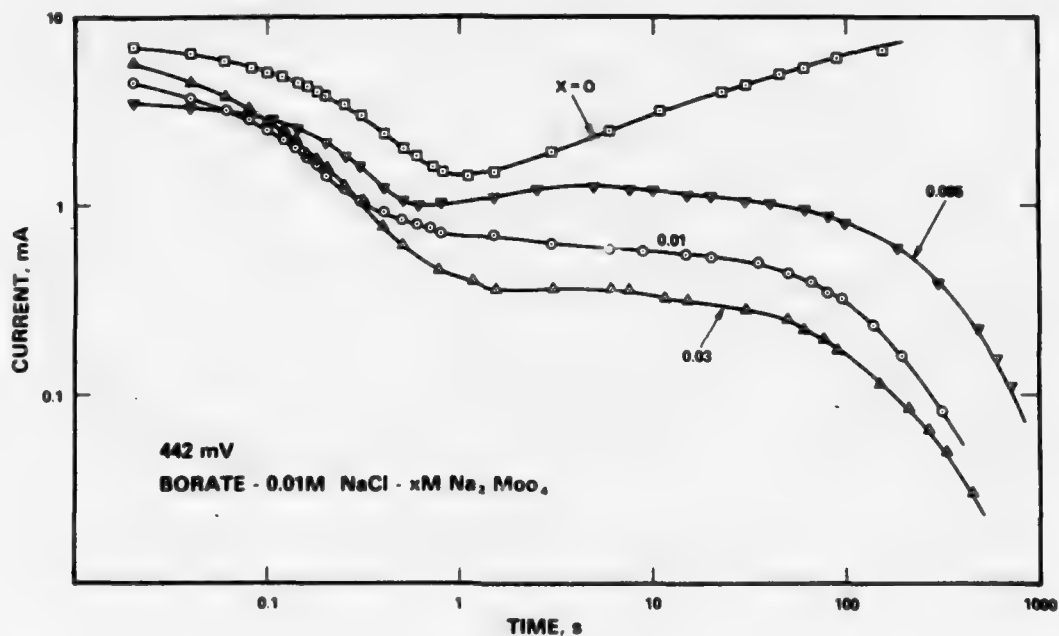
-18-

Fig. 8. Plot of anodic current decay against the logarithm of time in seconds for 4 concentrations of sodium molybdate, 0, 5 x 10^{-3}, 10^{-2}, 3 x 10^{-2} M. Repassivation occurs at 442 mV SHE in the sodium borate-boric acid buffer, chloride ion concentration = 10^{-2} M [from (1)].

-19-

REFERENCES

1.   T. Kodama and J. K. Ambrose, submitted to Corrosion, 1976.

2.   N. D. Tomashov, G. P. Orernova, and O. N. Marcova, International Conference on Localized Corrosion, Williamsburg, Va., 1971 NACE-3 (Houston, 1974) 363.

3.   W. Robertson, J. Electrochem. Soc. 98, 94 (1951).

4.   M. Pryor and M. Cohen, J. Electrochem. Soc., 100, 203 (1953).

5.   H. Goldschmiedt, Paint Manuf., 45, 22 (1975).

6.   Y. Fukase, K. Osozawa, R. Aemoto, Japan - U. S. Seminar on the Physical Metallurgy of Heat Resisting Alloys, Diamond Park, New York (1972).

7.   G. A. Lizlovs, Corrosion, 32, 263 (1976).

8.   J. R. Ambrose and J. Kruger, Corrosion, 28, 30 (1972).

9.   J. C. Scully, The Theory of Stress Corrosion Cracking in Alloys, NATO Science Committee, Brussels, (1971), 1.

10. J. R. Ambrose and J. Kruger, Technical Summary Report No. 5, NBSIR 74-583 (1974), 1.

11. J. J. Carroll and A. J. Melmed, Surface Science, 16, 251 (1969).

12. J. B. Lumsden and R. W. Staehle, Scripta Metallurgica, 6, 1205 (1972).

REPASSIVATION KINETICS OF MECHANICALLY DEPASSIVATED

METAL WITHIN A CREVICE

Introduction

One of the problems associated with any study into what factors are important in controlling susceptibility to crevice corrosion is that one must wait out some incubation period before measurable attack has begun. And it can well be that during this period subtle changes are occurring within the crevice - the solution, the films, the metal itself - that play a critical role in what will happen following some breakdown in passivity. For this reason, a technique which allows metal exposed to a crevice to be quickly depassivated after any elapsed exposure interval is necessary if one wishes to know what is really happening during the initial stages of crevice corrosion attack.

This work deals with the development of a technique which utilizes a pointed sapphire rod to scratch the surface of a metal electrode exposed within a crevice. Following this mechanical depassivation, repassivation kinetics can be measured using conventional electrochemical techniques. To date, first generation alterations in the original concept of the device have been made; these changes have led to a new type of crevice electrode. Other results have led to criteria of performance which will be carried over into any second generation design.

Experimental

The device used to measure repassivation kinetics of metal within a crevice basically consists of a female standard taper ground glass joint, the side arms of which have been modified for use as the elements of an electrochemical cell. In these side arms are contained a reference electrode bridge, an auxiliary platinum electrode, and solution addition/drain stopcock. In the same arm as the counter electrode is the sapphire tip assembly. Pressure to push the tip against the specimen is applied with a stainless steel spring, held in place by a Swagelok cap. The assembled cell is shown in Fig. 1.

The original crevice electrode is shown in Fig. 2. It is a 304 stainless steel plug machined to the specifications of a standard 19/38 taper and designed to fit the glass cell. This electrode as shown has been masked off with glyptal varnish to reduce the area of electrode actually in contact with the crevice electrolyte.

A new electrode design has been used in the studies presently underway. It incorporates a metal electrode section sandwiched between two pieces of teflon. The unassembled and assembled electrodes are shown in Figs. 3 and 4.

The dimensions of the crevice are controlled by the vertical position of the electrode in the crevice. This position is adjusted using the wheel around the threaded central shaft of the electrode. Mechanical depassivation is accomplished by rotating the electrode assembly in the crevice. Using a potentiostat, current decay during repassivation can be recorded on an oscilloscope; longer transients are more conveniently measured on a strip chart recorder.

Repassivation kinetics measurements of AISI 304 stainless steel in sodium chloride solutions are currently in progress.
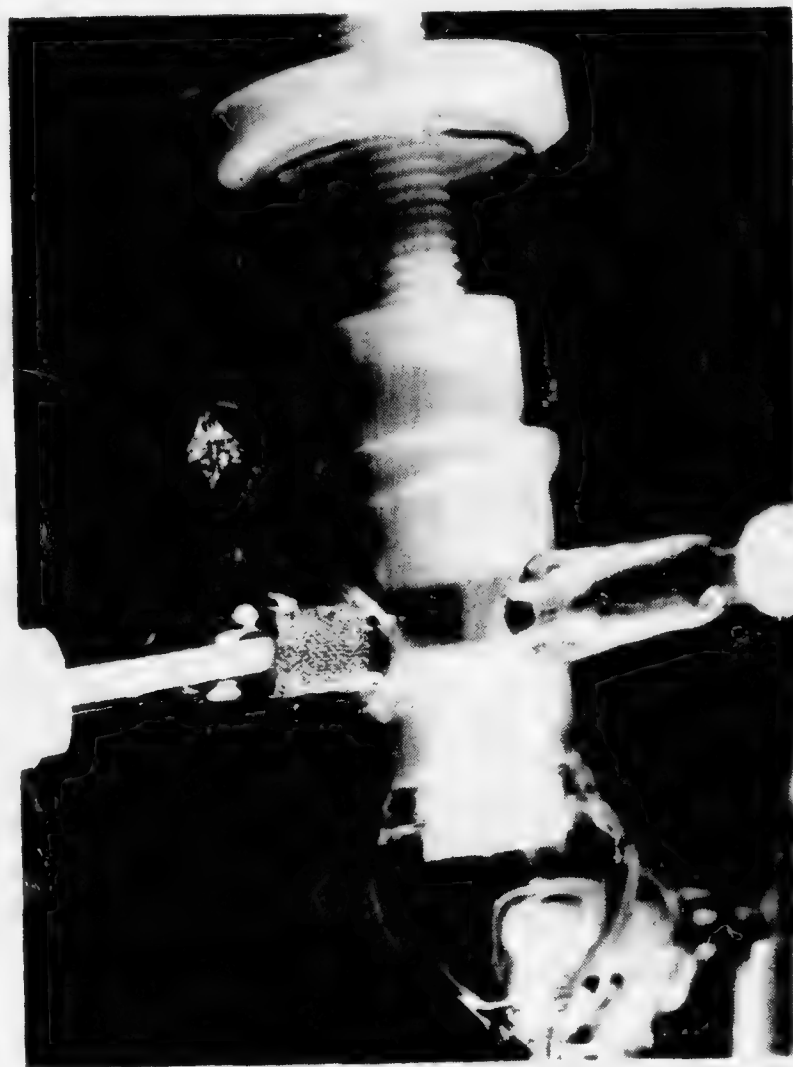
Fig. 1. Assembled cell for determination of repassivation kinetics for mechanically depassivated material within a crevice.
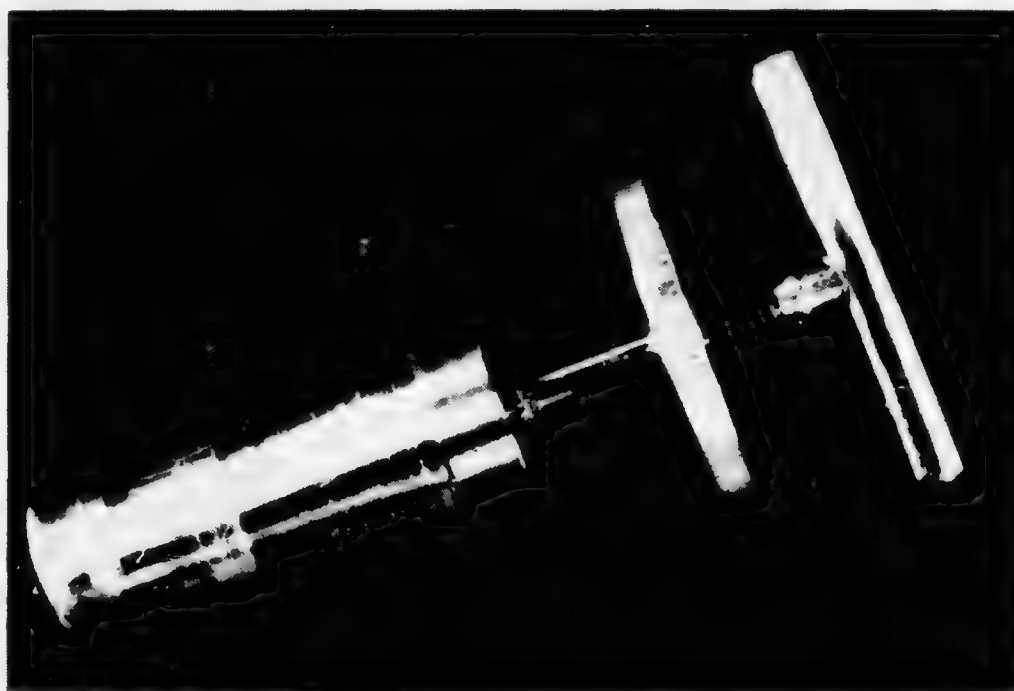
Fig. 2. Original machined 304 stainless steel electrode. Most of the exposed surface has been coated with laquer to reduce contact with the environment.
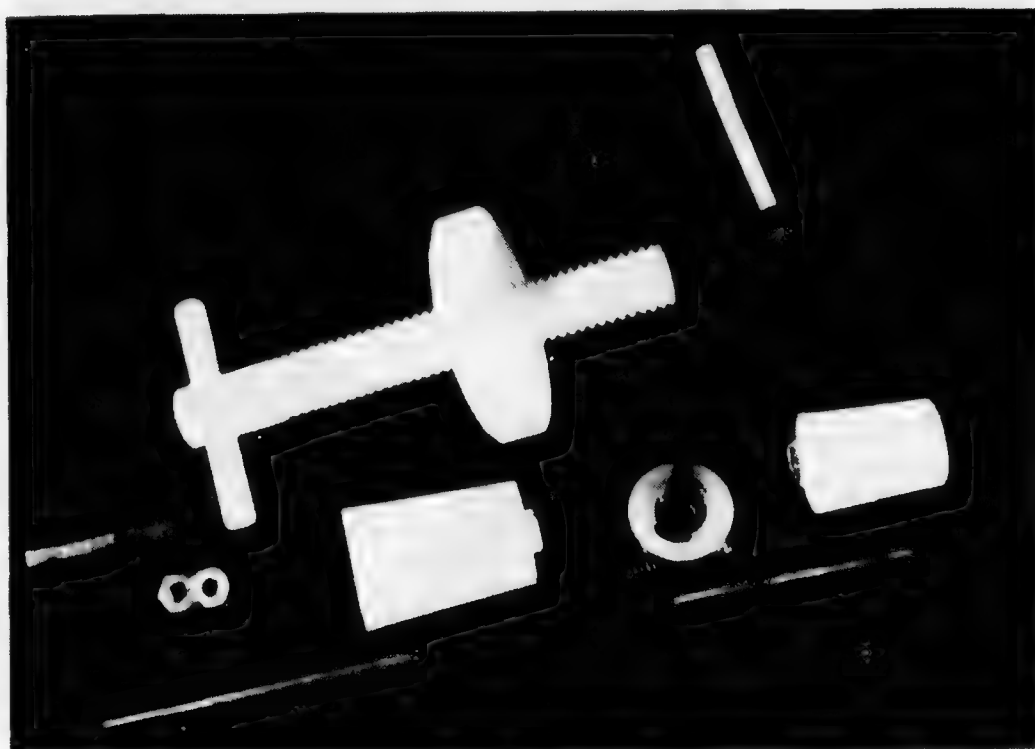
-24-

Fig. 3. Unassembled electrode used in crevice repassivation studies.
Shown are sapphire scratching device, metal specimen and the
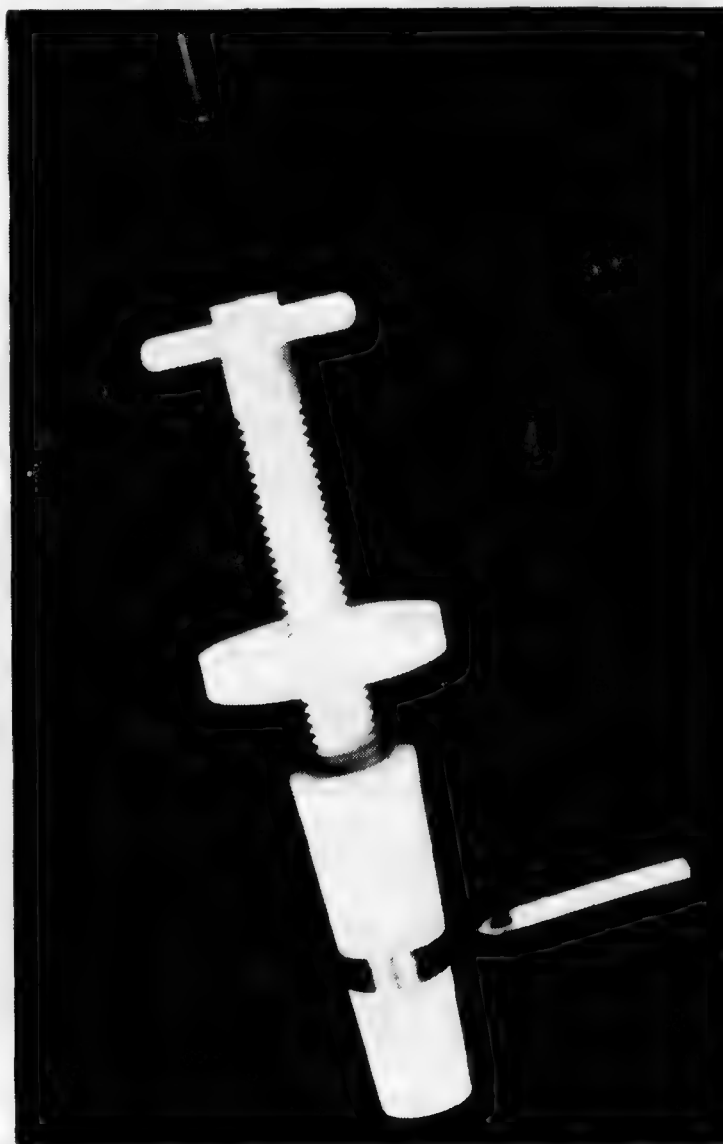teflon sections used to assemble the electrode.

Fig. 4. Assembled crevice electrode used in crevice repassivation measurements.

-26-

REPASSIVATION KINETICS OF SIMULATED CHROMIUM DEPLETED

ZONES IN AUSTENITIC STAINLESS STEELS

Introduction

Susceptibility of austenitic stainless steels to intergranular stress corrosion cracking (ISCC) during exposure to high temperature, high purity nuclear reactor water systems has been attributed to the presence of heat affected areas where the steel has been sensitized during welding (1). Sensitization has been said to result when formation of chromium carbide deposits ($Cr_{23}C_6$) in the grain boundaries leave an adjacent area of rather active zones where chromium has been depleted (2). Although extent of sensitization has been found to be related to susceptibility of this alloy to ISCC for materials which have been furnace sensitized, there has been great difficulty in establishing similar definite relationships for material which has been sensitized through welding alone (3). In other words, sensitization is a necessary but not sufficient condition to account for the susceptibility of austenitic stainless steels for ISCC. If, then, conventional time to failure stress corrosion cracking tests are not reliable indicators of material susceptibility, a need exists for a technique by which such susceptibility can be ascertained.

It has been suggested that a relationship exists between the rate at which a bare metal surface will repassivate and the susceptibility of that metal to stress corrosion cracking in that particular environment. In a previous study we have demonstrated the existence of that relationship for AISI 304 stainless steel as a function of pH and applied potential (3). Since chromium depletion is thought to result in a decrease in the protectiveness of the passive film on this particular steel, it was thought that the technique used then would be equally applicable now. This technique, tribo-ellipsometry, permits simultaneous measurement of film growth and current decay kinetics during the repassivation transient which follows surface film removal by mechanical abrasion (4).

This study will focus on the effect of systematic chromium depletion on repassivation kinetics of a series of Fe-10Ni-xCr where x varies from 18 to 3 weight percent. Along with these measurements, cathodic reduction kinetics studies will be made on a specimen of $Cr_{23}C_6$, the precipitated carbide found in grain boundaries of sensitized stainless steels.

To date, only the specimen preparation stage of the study has been completed.

Experimental Simulated Chromium Depleted Zones

To determine what effect selective depletion would have on the rate at which these materials would repassivate, a series of ternary Fe-10

Ni-xCr alloys were prepared in which the chromium concentration was varied betwen 3 and 18 weight percent. These prepared alloys are intended to simulate the chromium depleted regions produced during the sensitization process. Considerable effort was made to retain the austenite structures in all alloy compositions through variation in cooling rates and in carbon and nickel compositions, but the structure of the final alloy series consists of a martensite-like phase in a ferritic stainless steel matrix.

The compositions prepared were as follows:

Fe 18 W/O Cr   10 W/O Ni   only specimen austenitic in structure
Fe 15 W/O Cr   10 W/O Ni
Fe 12 W/O Cr   10 W/O Ni
Fe 9 W/O Cr   10 W/O Ni
Fe 6 W/O Cr   10 W/O Ni
Fe 3 W/O Cr   10 W/O Ni

Stoichiometric compositions of the above alloys were carefully weighed out using the highest purity materials available.

About sixty grams of each alloy was weighed out and then melted in the arc furnace under titanium gettered argon. The alloy was melted a minimum of four times on each side with the sides being alternated consecutively. After a total of eight meltings the alloy is in the shape of a hemispherical button and is then arc cast into an approximately square rod.

After the alloy was cast into a rod, it was removed from the arc furnace and mechanically deformed and shaped into a round rod by swaging to the desired diameter.

The alloy was then heat treated for the purpose of homogenization, stress relief and recrystallization of the as cast structure.

The heat treatment went as follows. The specimens were sealed in an evacuated vycar tube heat treated at 1000 °C overnight and quenched in ice water in the morning.

Ambient temperature repassivation kinetics measurements using a modification of the tribo-ellipsometric technique are presently in progess.

Chromium Carbides, $Cr_{23}C_6$

This material was prepared by F. S. Biancaniello of the Alloy Preparation Laboratory, Metallurgy Division, National Bureau of Standards.

$Cr_{23}C_6$ has a cubic, $D8_4$ type of structure, a=10·638kX, D_m=6·97 g/cm^3 M=4, Fm3m. This phase was earlier referred to as Cr_4C.

Stoichrometric quantities of chrome pieces (varying from -100 mesh up to about 0.5 grams) and carbon (lamp black fine powder) were weighed out and placed in an alumina crucible which was placed in the Balzers vacuum, melting and casting induction furnace for overnight pumpdown.

The following day the charge was heated to about 800 °C to drive off any moisture that may have remained in the system. Then, gettered argon was introduced to the system to a pressure of five hundred torr.

Finally, the charge was melted and held molten about twenty minutes with the power reduced gradually until solid began to form at which time the specimen was held at temperature about ten minutes. Power was then turned off entirely and the specimen allowed to furnace cool.

Metallographic examination indicated that there was present less than one percent secondary phase present in the prepared compound. The primary phase was confirmed by x-ray examination to be $Cr_{23}C_6$.

REFERENCES

1. C. S. Tedmon, Jr., D. A. Vermilyea, and J. H. Rosolowski, J. Electrochem. Soc., 118, 192 (1971).

2. R. L. Cowan, II and C. S. Tedmon, Jr., "Intergranular Corrosion of Iron-Nickel-Chromium Alloys", General Electric Report No. 72CRD298, Technical Information Series, October 1972.

3. A. E. Pickett, Stress Corrosion Tests of Reactor Structural Materials in Simulated BWB Environments, General Electric Report NEDE-13179, April 1971.

4. J. Kruger and J. R. Ambrose, Technical Summary Report Number 4, NBSIR 73-244, "The Role of Passive Film Growth Kinetics and Properties in Stress Corrosion and Crevice Corrosion Susceptibility", 1973.

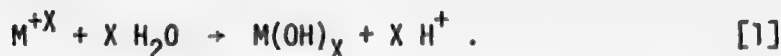5. J. R. Ambrose and J. Kruger, Corrosion, 28, 30 (1972).

PART IV

NEW APPROACHES TO THE STUDY OF LOCALIZED CORROSION

Jerome Kruger
Institute for Materials Research
National Bureau of Standards
Washington, D. C. 20234

A number of approaches have been developed over the years to study localized corrosion. This paper will single out some of the newer approaches that have attempted to focus on a number of relevant issues that must be always borne in mind if one wishes to obtain a valid under-standing of local corrosion processes. This paper will not review all the relevant issues, nor will it be an all-inclusive description of the various new ways in which localized corrosion can be studied. Instead, it will mostly concentrate on the results of some experimental approaches that have had an influence on changing some of the ways localized corrosion has been considered in the past. This paper is not intended as a comprehensive look but rather a more narrow, personal, and, perhaps, opinionated enumeration of important issues to be considered when study-ing localized corrosion.

RELEVANT ENVIRONMENTS

One of the major reasons why many studies of localized corrosion have failed to reveal important insights into the processes controlling such corrosion has been the failure to use relevant environments. This is so because localized corrosion usually takes place within the restricted confines of a crack, a pit, or a crevice. Because diffusion of ions in or out of the confines of this restricted space (called by B. F. Brown an "occluded cell") is difficult, concentrations of these ions are built up or decreased. Thus, the environment within a pit is not that of the environment of the solution that exists outside the pit. Unfortunately, it is the environment outside the pit in which many workers choose to carry out experiments. For example, a very important reaction occurring in an "occluded cell" is the hydrolysis reaction that can lower the pH below that of the surrounding environment in the following way:

$$M^{+X} + X\ H_2O \rightarrow M(OH)_X + X\ H^+ . \qquad [1]$$

The relevant environment to be used in a study or to be considered in the interpretation of an experiment would be the one that takes the pH of the environment produced by reaction [1] into consideration.

While it has been recognized for a number of years that the environment trapped in the interior of restricted regions on a metal (cracks, pits, and crevices) has a different composition than the bulk environment surrounding the metal, it has been only in recent years that such knowledge was considered important, and serious attempts made to measure the composition of the occluded environment in a crack. (An important exception is the use of ferric chloride solutions of low pH to carry out screening tests of the resistance of alloys to pitting.) Brown and co-workers (1-3), using the insights provided by the large body of work of Pourbaix (see the review in (4)) that systematized the role of pH and potential in all corrosion processes, set about to measure these parameters in cracks. Their original approach was to immobilize the corrodent within stress corrosion cracks by freezing it in liquid nitrogen, breaking open the crack mechanically, and then analyzing the thawed out solution removed from the crack. A later development used microelectrodes to determine the pH and potential in the crack's environment. Other developments in this fast moving field have been the use of a capillary to sample the crack solution (5) and the combination of a capillary technique with thin layer chromatography (6) to examine the solution in crevices.

The value of these crack pit or crevice chemistry techniques becomes evident when Fig. 1 is inspected. It shows for a large number of steels of different compositions in environments of either high or low pH that the potential and pH inside the crack falls in a region of the pH potential diagram (Pourbaix diagram) where one expects both corrosion and, because the points on Fig. 1 are below the line marked H, the presence of hydrogen. Thus, any failure prevention measures using bulk composition or potentials could be based on non-realistic conditions and lead to an improper choice. A good discussion of the electrochemical ramifications of knowing the proper environment in a crack is given by Pourbaix (4).

RELEVANT ALLOY STRUCTURE AND COMPOSITION

In many cases of localized corrosion, differential rates of attack for the different phases present in an alloy are observed. For example, the difference in potential between the phase making up a grain boundary (or grain boundary region) and the interior of a grain may be the driving force for intergranular corrosion. A similar situation can exist when pitting or stress corrosion is observed. Thus, it becomes important, when one wishes to disentangle the origins of localized attack, to study in detail the process occurring on the individual phases. A fruitful approach is to study, for example, the electrochemistry of alloys that are identical or similar to the relevant phases that make up the different regions of a real alloy whose localized corrosion one seeks to understand.

Figs. 2 and 3 from some work by Ugiansky (7) show the kind of results that can be obtained with such an approach. The anodic polarization curves carried out in a 1.0 M NaCl, pH 7, O_2 free solution on

alloys simulating three important phases or regions found on Al-Zn-Mg alloys (Fig. 2) show only minor differences between the electrochemical behavior of the precipitate phase in the grain boundary, the precipitate free zone (PFZ) which occurs near the grain boundary in the real alloy, and the grain interior matrix. When 1.0 M $NaNO_3$ is substituted for 1.0 M NaCl (Fig. 3), however, the three alloys simulating the different regions in a complete alloy exhibit markedly different electrochemical behavior; the precipitate phase that exists in the grain boundary exhibits current densities (corrosion rates) that are over three orders of magnitude higher that the other two phases examined. Thus, the approach of studying relevant alloys (in this case simulating the different phases or regions of an Al-Zn-Mg alloy) has yielded valuable insights into the origins of intergranular attack of such alloys.

Not only are different phases or compositions important, but also structural variations, such as different crystallographic orientation of the grains of a metal or the presence of variations, for example, dislocations, within the same orientation, can be a factor underlying localized attack. For example, studies by Kruger (8) on single crystal iron surfaces showed that pitting was more predominant on surfaces whose orientations were near the {110} orientation than on those of other orientations (Fig. 4). This example illustrates the kind of information one can gain by working with surfaces of known structures. By knowing the orientation of the surface one is examining, one can determine which are the relevant structures that affect the localized corrosion processes whose origins are being unraveled.

RELEVANT CRITICAL POTENTIALS

There are vast numbers of experiments and discussions (9-13) in the literature on the factors or underlying causes of the existence of a critical potential for pitting and for stress corrosion. This is so because the concept of a critical potential, E_c, below which localized attack does not occur has immediate practical consequences. Obviously, if one knows E_c for a given alloy and environment one then has a great incentive to control the potential of that system so that it never goes above E_c and thereby, presumably, never suffers localized attack. One does, however, have to know the relevant E_c. It is because the relevant E_c is not always known because it is measured incorrectly that the concept of a critical potential is held in disrepute by some workers (9). Even if one can measure a relevant E_c, it is by no means established that all pitting or stress corrosion will be stopped by keeping a system below E_c. Nevertheless, one can never establish the practical validity of the concept until it is assumed that the correct, that is, relevant value of E_c is used.

How is the relevant E_c determined? The answer to this question depends on what process or phenomenon determines the value of E_c.

Unfortunately, this has not been established although a number of suggestions have been advanced (14). The different explanations of the origin of E_c can be listed as follows:

a) E_c determined by potential of zero charge - Almost all mechanisms of localized corrosion require as their first step the adsorption of damaging anions. Roughly, the potential above which such adsorption takes place is the potential of zero charge (pzc). Thus, since some mechanisms for pitting require that damaging anions adsorb and thereby displace the ions forming the passive film, such an explanation of E_c would be reasonable, and the effect of such variables as the nature of the metal, concentration of anions, and temperature all affect E_c and pzc (see 15,16). Because it is difficult to measure the pzc for solid electrodes (15) especially when adsorption may coincide with the initiation of breakdown processes, there have been no good experimental verifications that E_c is related to the pzc.

b) E_c is determined by film pressure to fracture film - Sato (17) has identified E_c with the critical potential above which the film pressure exceeds the critical compressive stress of film mechanical breakdown. The film pressure depends upon both electrostriction and interfacial effects.

c) E_c is determined by the potential of formation of an unprotective film - One possible factor determining E_c which may not apply to all cases may be that it is the potential above which an unprotective film may form or deposit. Ambrose and Kruger (18) suggest that this may be the case for iron.

d) E_c is determined by repassivation kinetics - This concept of E_c is based on kinetic considerations. Some studies (19-22) have suggested that a competition between repassivation and breakdown of films is important in determining initiation of localized attack. Videm (19) has proposed that the value of E_c for Al is determined by the relative rates of these two processes. He based this on his experiments that showed a narrow potential region where repair and breakdown were competitive. Below this region, repair predominated and above it, breakdown was the major process. Because potential can affect repassivation kinetics (23,24) and because, a number of workers (20-22,25,26) suggest, initiation of localized attack depends on a dynamic balance between breakdown and repair, the determination of E_c by repassivation kinetics is a possibility to be considered. (More will be mentioned about repassivation in the section on Relevant Basic Processes.)

Thus far, it is explanation d) that has led to new approaches for determining E_c. These show some promise at yielding more relevant values. Notable among these approaches is that of Pessel and Liu (13). Their technique involves scratching the alloy surface whose E_c is to be

determined at various potentials set by a potentiostat in the environment under examination.* When the potential is below E_c, the current observed upon scratching rapidly returns to the original values observed before scratching. When the potential is above E_c, no or very little repassivation occurs and the current either remains near the value found after scratching or it increases. Fig. 5 shows the kind of current transients observed above and below E_c. A major advantage of this approach is that it eliminates the induction time for localized corrosion to be initiated. The usual methods for determining E_c do not have this virtue. With the common methods one may either scan potentiodynamically a potential region or potentiostatically sample a series of potentials in succession staying at each potential for varying amounts of time. When a value for the potential is reached at which the current measured starts to increase, this value is identified as E_c. However, it is known that there exists an induction time for localized corrosion attack. Therefore, unless one stays at all potentials for a time greater than the induction time, one can never be assured that a lower potential would not have been E_c. Since the induction time can be very long depending on the history of the sample studied (see Ambrose and Kruger (18)), it is no wonder that the E_c determined by the usual methods has been considered by some to be of questionable value (9). Because Pessel and Liu's technique eliminates the problem of time of initiation, it appears that the E_c determined by its use is a more relevant value.

Likewise, the potential identified by Pourbaix (11) as the protection potential, E_p, may also be more relevant. This potential, which is more active than E_c, is the potential below which localized corrosion once started can be stopped. Pessel and Liu's work indicates that when E_c is determined by their technique, a way that eliminates the time for initiation of attack to occur, $E_c = E_p$.

RELEVANT BASIC PROCESSES

In the preceding section a technique for determining E_c was considered to give relevant values because it was based on the supposition that repassivation was a process strongly affecting localized attack. A number of workers (19-21) have suggested that the rates of two major basic processes, breakdown of passivity and repassivation, are of great importance in determining whether localized attack will occur. By focusing on these two basic processes, breakdown and repairs, some valuable approaches have been developed for studying localized corrosion.

---

* Actually a more relevant environment would be that environment one would expect to develop in a pit, crack, or crevice when the surface is exposed to the ambient environment.

-35-

One technique that has been suggested as actually looking at breakdown-repair events is that concerned with examining the small fluctuations of potential or current occurring on a corroding surface, "noise". Iverson (27) showed that the frequency and intensity of such noise could be markedly diminished by the addition of an inhibitor to a corroding system (Fig. 6). Videm (19) and Okamoto et al. (28,29) have suggested that the noise represents breakdown and repassivation events and that the dynamic competition between these two basic processes determines whether localized attack such as pitting will be initiated. The function of the chloride ion in pitting is to tilt the scale towards breakdown and corrosion by slowing down or stopping effective repassivation (19,21).

If repassivation kinetics is, therefore, an important basic process, attention must be focussed on it and ways developed to separate its measurement out from the breakdown process that always occurs along with it during localized corrosion. Scully (30,31) was one of the earliest workers to emphasize the importance of repassivation kinetics, and it has become an important element, especially in the film rupture metal-dissolution mechanism of stress corrosion (SCC), because combined with the concept of slip step dissolution, it explains why restricted lateral dissolution occurs - the slower the repassivation, the more of the metal slip step that has emerged and ruptured the film can be dissolved before new film forms. If too little dissolves, no SCC occurs; if too much dissolves, the dissolved areas are not restricted enough, and the crack is too blunt to propagate. Only when the environment and alloy provide a system where the repassivation kinetics produce a highly restricted region for dissolution is SCC found. In addition to Scully, Staehle (32) has given a detailed discussion of the significance of repassivation kinetics.

These considerations have resulted in a number of techniques aimed at determining the repassivation kinetics (33-38). These techniques produce a bare surface either by straining an alloy wire or by scratching or abrading a surface. In most of these techniques, the specimens are either strained or scratched while maintaining their potentials at a fixed value and measuring the current transient that takes place during the dissolution-repassivation event that occurs subsequent to exposure of bare metal. The rate of current decay is related to the rate of repassivation. A new and useful technique for measuring susceptibility to SCC by looking at repassivation kinetics is that developed by Galvele et al. (39). This technique determines anodic and cathodic polarization curves for both an unstrained and strained electrode. The ratio between the corrosion current for the unstrained electrode to that of the strained can then be used to assess susceptibility.

In such mainly electrochemical techniques, one cannot separate out the current involved in dissolution from that involved in passive film formation. Using a technique developed by Ambrose and Kruger (38), however, it is possible to measure separately the film regrowth transient

-36-

by optical means (ellipsometry) and to compare it to the overall dissolution-repassivation current. With this technique, called tribo-ellipsometry, one removes the protective film on a metal in an environment by means of a polishing wheel and then records both the film growth kinetics and the current as shown in Fig. 7. In Fig. 7 we can see that the rate of film growth on a titanium alloy is considerably slower in the susceptible chloride environment than it is in the nonsusceptible nitrate solution. With tribo-ellipsometry one can determine the ratio of the total current to that involved in repassivation only. This ratio R_p* when the exposed surface area is known is given by the expression

$$R_p^* = 1 + \frac{Q_d}{Q_r} \qquad [2]$$

where Q_d = charge involved in dissolution and Q_r = charge involved in repassivation.

R_p* is a measure of the effectiveness of the repassivation process. Work on the cracking of low carbon steel (40) has shown that SCC does not occur when the effectiveness of repassivation is either too high or too low. Thus, for low carbon steel, at the time required to form a complete film, R_p* is 2.8 in 1 N $NaNO_2$ (25 °C) where it is nonsusceptible; R_p* is 26 in 4 N $NaNO_3$ (90 °C) where it does undergo SCC, and R_p* is > 75 in 1 N NaCl (25 °C) where it undergoes widespread pitting attack but not SCC. Thus, a delicate balance between repassivation and dissolution must be maintained to lead to SCC. The determination of this balance is dependent on the environment, the alloy, and finally the metallurgy and mechanics of the system that control the rate at which bare metal sites (generally slip steps) are produced as well as their density and size.

It is on the rate at which bare metal sites are produced that another new approach to localized corrosion (primarily SCC) is based. This approach uses the constant strain rate technique which gives some information on the beneficial breakdown processes occurring in SCC. This technique, which produces experimental data as depicted in Fig. 8, can be applied both to mechanistic studies as well as used for routine testing. The mechanistic importance of the technique is that it ties the metallurgically controlled rate of bare metal exposure, resulting from film rupture by slip step emergence, to the chemical process of repassivation of the exposed metal. This can be seen by examining the significance of the three regions shown in Fig. 8. For Region A where strain rates are too low to lead to SCC, the rate of repassivation is high enough to prevent any significant and damaging interaction between the environment and the bare metal exposed during straining. At the opposite extreme, Region C, the strain rate is so rapid that the inter-action of the exposed metal with the environment is of no consequence because the rate that the metal fails by ductile fracture exceeds the rate by which the environment can affect fracture via any of the possible SCC mechanisms (dissolution, hydrogen embrittlement, or adsorption of damaging species). It is only in the intermediate range of strain rates, Region B, where the rate of production of bare metal sites has a

value sufficiently high so that the rate of repassivation does not prevent environmental access. However, the strain rate is sufficiently low so that environmental interaction and not ductile pulling apart produces fracture. Under these conditions SCC takes place. If SCC is not possible for the system studied, the dip shown in Region B will not occur.

Does this test, whose development and increasing use was stimulated for mechanistic reasons and was mainly guided by the implications of film rupture and repassivation, provide a valid routine material-environmental evaluation test? Parkins (41) has pointed out that there are certain features of the constant strain rate technique that make it a useful routine laboratory test. These features are as follows:

(1) It is a relatively severe test so that it will promote laboratory SCC failures where other tests on smooth specimens will not unless inordinately long testing times are used;

(2) It always produces fracture by SCC or some other mechanism and therefore is a positive test;

(3) The time of testing is relatively short.

These three somewhat interrelated attributes, severity, positiveness, and rapidity, are especially valuable in comparative testing where one wishes to intercompare materials and environments.

The promise that the constant strain rate approach offers for laboratory testing is somewhat tempered by the lack of good ways to quantify the results of the tests. For example, how does one relate the strain rate in Region B where SCC susceptibility is the greatest to crack growth rate? Moreover, it is not known what relation, if any, this strain rate bears to the strain rate that exists at the tip of a growing crack. Parkins (41) has made some valuable qualitative connections between this value and the threshold stress for SCC or the threshold value of the stress intensity factor (an important parameter in the fracture mechanics approach to SCC testing (42)) but the quantitative relationships require new theoretical and experimental advances. Despite these problems, the constant-strain rate tests have provided evidence of SCC in systems where other tests have been difficult or not possible to apply (43-46).

RELEVANT FILMS

The protective films that form on alloy surfaces in a given environment are of crucial importance in controlling localized attack because their ability to withstand the breakdown processes determines whether such attack will occur. In attempting to determine how these films affect localized attack one must be sure that certain relevant considerations with respect to the film's ability to affect localized

-38-

corrosion are borne in mind. Three such important, but not all-inclusive, considerations will be suggested here, 1) pretreatment, 2) structure, and 3) origin.

The first consideration, pretreatment, is concerned with the history of the film prior to its exposure to an environment that causes localized attack - generally one containing aggressive anions. It is because this consideration is ignored that potentiodynamic scans lead to erroneous values of E_c, as discussed in an earlier section. This is so because pretreatment can markedly affect the time required to initiate break-down. For example, Ambrose and Kruger (18) showed that annealing the passive film on iron at 65 °C for one hour and then bringing the system back to room temperature, increased the induction time over 100-fold. Therefore, they reasoned that the defects in the film, through which penetration must proceed, were removed by the annealing. Similar results for Ta were found by Vermilyea (47). Fig. 9 shows, by using the technique of ellipsometric spectroscopy (48), that the annealed films on iron exhibit entirely different optical changes when exposed to Cl^- ions. It is thus obvious that the relevant film to be considered in a study of localized corrosion is the one whose pretreatment history is known.

Pretreatment by annealing does not always increase the time for localized corrosion initiation to occur. Unlike the situation for iron, as just described, Okamoto (22) found that annealing the passive film on stainless steel shortened the induction time for the initiation of pitting. The reason for this entirely opposite behavior for stainless steel as compared to iron lies in the second consideration, film structure. The passive film on stainless steel is noncrystalline or "glassy" (22,49) and such a glass-like structure provides few diffusion paths for pene-tration by aggressive anions. When annealed, however, the noncrys-talline structure of the passive film on stainless steel can crystallize and the new grain boundaries formed offer greater opportunities for diffusion. It can thus be seen that one has to consider the structure of the relevant passive film in studying localized corrosion.

The influence of alloy composition on structure and composition of the passive films is intimately tied in with the third consideration, the origin of the film; or more precisely, does the relevant film being considered come from growth on the alloy or from precipitation or formation from the environment? To illustrate the point that is being made, consider the problem that although Mo in a stainless steel is known to be beneficial in preventing or retarding pitting or crevice corrosion, recent work (50,51) has shown that it is not present in the passive films formed in such alloys. Its beneficial effect can only come from its effect on propagation rather than on initiation where the initial passive film properties are important. Streicher (52) has shown this to be so and recent repassivation kinetic studies by Kodama and Ambrose (53) found that Mo may be involved in inhibiting pit propagation by precipitating a protective layer of ferrous molybdate from solution, the

molybdate being formed when some of the alloy goes into solution during pit initiation. Thus, the relevant protective film affecting localized corrosion is not the original film formed by passivation of the alloy surface but a film whose origin is a precipitation reaction occurring in solution between ions that were formed during the initiation stage.

CONCLUDING REMARK

A fruitful study of localized corrosion requires the same weeding out exercise required in watching some modern or *avant garde* plays. Unless one separates out the relevant characters (relevant environment, alloys, potentials, films) from those that do not matter and follows the relevant plot lines (relevant basic processes), one will not get much out of the play, nor will one get much understanding of the localized corrosion process being studied.

ACKNOWLEDGMENT

REFERENCES

1. B. F. Brown, C. T. Fujii, and E. P. Dahlberg, J. Electrochem. Soc., 116 218 (1969).

2. G. Sandoz, C. T. Fujii, and B. F. Brown, Corrosion Sci., 10 839 (1970).

3. J. A. Smith, M. H. Peterson, and B. F. Brown, Corrosion, 26, 539 (1970).

4. M. Pourbaix, Theory of Stress Corrosion Cracking of Alloys, J. C. Scully, Editor, NATO, Brussels, p. 17 (1971).

5. H. Leidheiser, Jr., and R. Kissinger, Corrosion, 28, 218 (1972).

6. F. D. Bogar and C. T. Fujii, Naval Research Laboratory Report 7690, March, 1974.

7. G. M. Ugiansky, Dissertation, Ohio State University, 1976, to be published.

8. J. Kruger, J. Electrochem. Soc., 106, 736 (1959).

9. M. J. Pryor, Localized Corrosion, Staehle, Brown, Kruger, and Agrawal, Editors, NACE, Houston, p. 2 (1974).

10. B. E. Wilde, Localized Corrosion, Staehle, Brown, Kruger, and Agrawal, Editors, NACE, Houston, p. 342 (1974).

11. M. Pourbaix, Localized Corrosion, Staehle, Brown, Kruger, and Agrawal, Editors, National Association of Corrosion Engineers, p. 12 (1974).

12. S. Smialowska and M. Czachor, Localized Corrosion, Staehle, Brown, Kruger, and Agrawal, Editors, NACE, Houston, p. 353 (1974).

13. N. Pessall and C. Liu, Electrochemica Acta, 16, 1987 (1971).

14. J. Kruger, Proc. Passivity and its Breakdown on Iron and Iron Base Alloys, R. W. Staehle and H. Okada, Editors, NACE, Houston, p. 91 (1976).

15. J. O'M. Bockris and A. K. N. Reddy, Modern Electrochemistry, Vol. 2, Plenum Press, New York, p. 706 (1970).

16. S. D. Argade and E. Gileadi, Electrodeposition, E. Gileadi, Editor, Plenum Press, New York, p. 87 (1967).

17.   N. Sato, Electrochemica Acta, 19, 1683 (1971).

18.   J. R. Ambrose and J. Kruger, Proc. 4th International Congress on Metallic Corrosion, NACE, Houston, p. 698 (1972).

19.   K. Videm, Kjeller Report KR-149, Institutt for Atomenergi, Kjeller, Norway (1974).

20.   J. Kruger and J. R. Ambrose, NBS Report NBSIR 74-583, September (1974).

21.   J. Zahavi and M. Metzger, Localized Corrosion, Staehle, Brown, Kruger, and Agrawal, Editors, NACE, Houston, p. 547 (1974).

22.   G. Okamoto, Corrosion Science, 13, 471 (1973).

23.   J. R. Ambrose and J. Kruger, Proc. 5th International Congress on Metallic Corrosion, NACE, Houston, p. 406.

24.   J. R. Ambrose and J. Kruger, J. Electrochem. Soc., 121, 599 (1974).

25.   J. R. Galvele, S. M. deMicheli, I. L. Muller, S. B. deWexier, and I. L. Alanis, Localized Corrosion, Staehle, Brown, Kruger, and Agrawal, Editors, NACE, Houston, p. 580 (1974).

26.   K. J. Vetter and H. H. Strehblow, Localized Corrosion, Staehle, Brown, Kruger, and Agrawal, Editors, NACE, Houston, p. 240 (1974).

27.   W. P. Iverson, J. Electrochem. Soc., 115 617 (1968).

28.   G. Okamoto, T. Sugita, S. Nishiyama, and K. Tachibana, Boshoku Gijustou, 23, 439 (1974).

29.   G. Okamoto, K. Tachibana, S. Nishiyama, and T. Sugita, Passivity and its Breakdown on Iron and Iron Base Alloys, R. W. Staehle and H. Okada, Editors, NACE, Houston, p. 106 (1976).

30.   J. C. Scully, Corrosion Sci., 7, 197 (1967).

31.   J. C. Scully, Corrosion Sci., 8, 513 (1968).

32.   R. W. Staehle, Theory of Stress Corrosion Cracking in Alloys, J. C. Scully, Editor, NATO, Brussels, p. 223 (1971).

-42-

33.   T. P. Hoar and J. M. West, Proc. Roy. Soc., 268A, 304 (1962).

34.   H. Leidheiser, Jr., and E. Kellerman, Corrosion, 26, 99 (1970).

35.   T. Murata and R. W. Staehle, Proc. 5th Intl. Cong. on Metallic Corrosion, NACE, Houston, (1974).

36.   N. D. Tomashov and L. P. Vershinina, Electrochimica Acta, 15, 501 (1970).

37.   J. R. Ambrose and J. Kruger, Corrosion, 28, 30 (1972).

38.   R. B. Diegle and D. A. Vermilyea, J. Electrochem. Soc., 122, 180 (1975).

39.   J. R. Galvele, S. B. deWexler, and I. Gardiazabal, Corrosion, 31, 352 (1975).

40.   J. R. Ambrose and J. Kruger, Proc. 5th Intl. Cong. on Metallic Corrosion, Tokyo, NACE, Houston, p. 406 (1974).

41.   R. N. Parkins, Theory of Stress Corrosion Cracking in Alloys, J. C. Scully, Editor, NATO, Brussels, p. 449 (1971).

42.   B. F. Brown, Ed., Stress-Corrosion Cracking in High Strength Steels and in Titanium and Aluminum Alloys, Naval Research Laboratory, U.S. Government Printing Office, Washington, 1972.

43.   W. R. Wearmouth, G. P. Dean, and R. N. Parkins, Corrosion, 29, 251 (1973).

44.   R. N. Parkins, F. Mazza, J. J. Royuela, and J. C. Scully, Brit. Corr. J., 7, 154 (1972).

45.   J. C. Scully and D. T. Powell, Corrosion Sci., 10, 371 (1970).

46.   D. C. Deegan and B. E. Wilde, Corrosion, 29, 310 (1973).

47.   D. A. Vermilyea, J. Electrochem. Soc., 104, 485 (1957).

48.   C. L. McBee and J. Kruger, Localized Corrosion, Staehle, Brown, Kruger, and Agrawal, Editors, NACE, Houston, p. 252 (1974).

49.   C. L. McBee and J. Kruger, Electrochemica Acta, 17, 1337 (1972).

50.   J. B. Lumsden and R. W. Staehle, Scripta Metallo, 6, 1205 (1972).

51.   C. L. McBee and J. Kruger, Passivity and its Breakdown on Iron and Iron Base Alloys, R. W. Staehle and H. Okada, Editors, NACE, Houston, p. 131 (1976).

52.   M. A. Streicher, J. Electrochem. Soc., 103, 375 (1956).

53.   T. Kodama and J. R. Ambrose, NBS Report NBSIR 75-916, October (1975). Submitted to Corrosion.

54.   B. F. Brown, Theory of Stress Corrosion Cracking in Alloys, J. C. Scully, Editor, NATO, Brussels, p. 197 (1971).
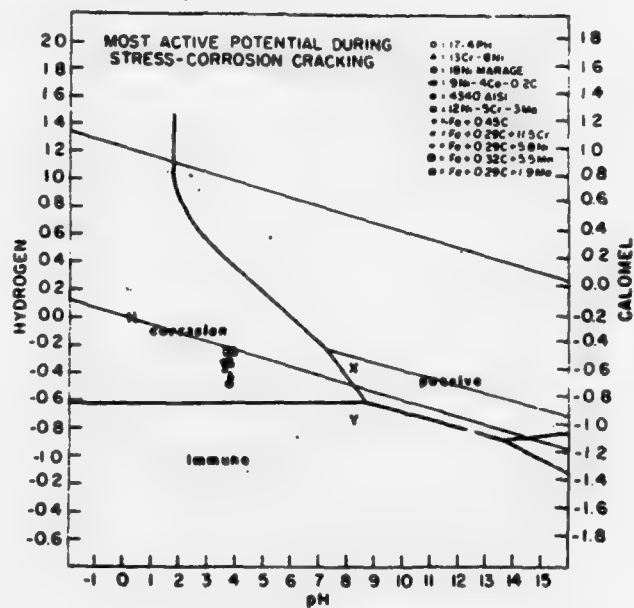
Fig. 1. Potential-pH diagram showing the potential-pH values in the
crack tip environments for a number of high strength steels.
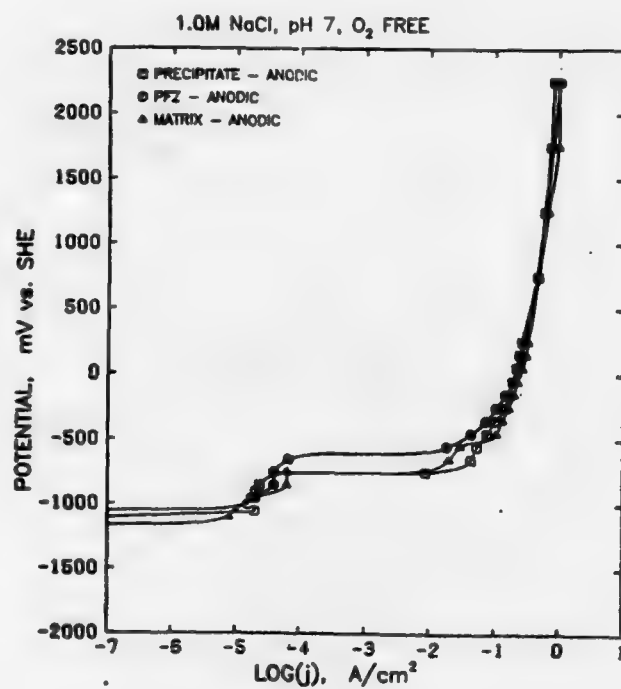From Brown (54).

Fig. 2. Polarization curves obtained in a 1.0 M NaCl solution, pH 7, O_2 free for different alloys simulating the various regions or phases existing in an Al-Zn-Mg alloy. From Ugiansky (7).
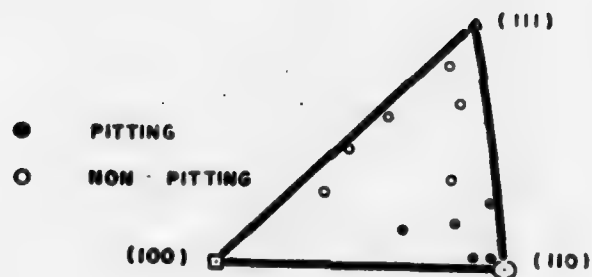
-46-

Fig. 3. Polarization curves obtained in a 1.0 M NaNO₃ solution, pH 7, O₂ free for different alloys simulating the various regions or phases existing in an Al-Zn-Mg alloy. From Ugiansky (7).

-47-

Fig. 4. Stereographic triangle showing pitting on grains of iron having different crystallographic orientations. From Kruger (8).

-48-

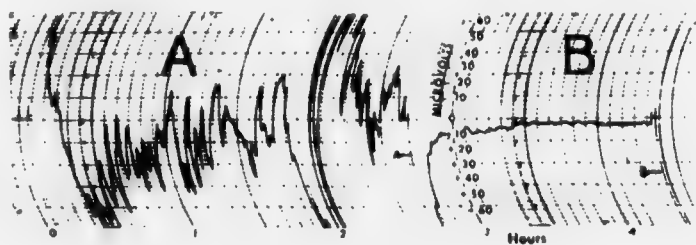Fig. 5. Scratch-test current-time curves for specimen held potentiostatically above E_C (breakdown) and below E_C (repassivation).

-49-

Fig. 6. Periodic potential fluctuations on A--a mild steel surface in
0.1% NaCl solution and B--after 1% NaNO$_2$ has been added to the
NaCl solution. Note how the inhibitor NaNO$_2$ reduces the pulse
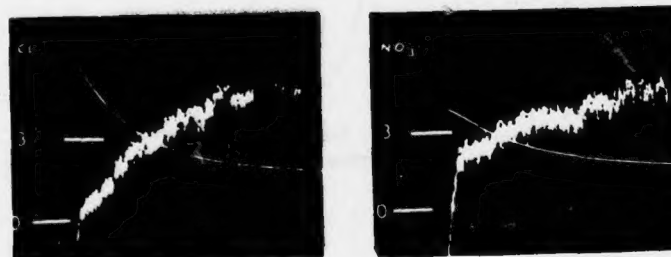intensity. From Iverson (27).

-50-

Fig. 7. A comparison of oscilloscope repassivation transients for Ti-8
         Al-1 Mo-1 V alloy in 1 N NaCl and NaNO$_3$ solutions at +706 mV (SHE)
         (ellipsometric film growth-jagged trace; current-solid trace).
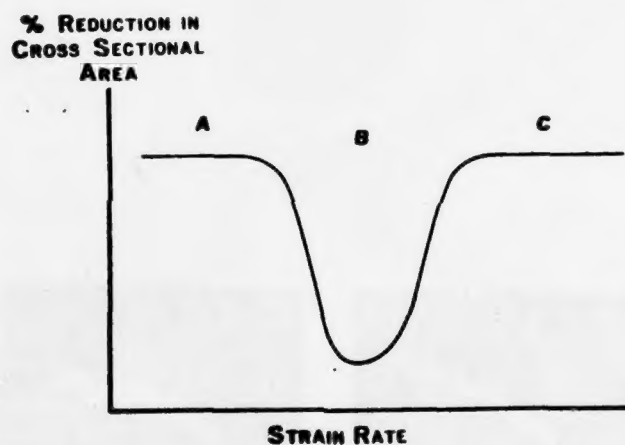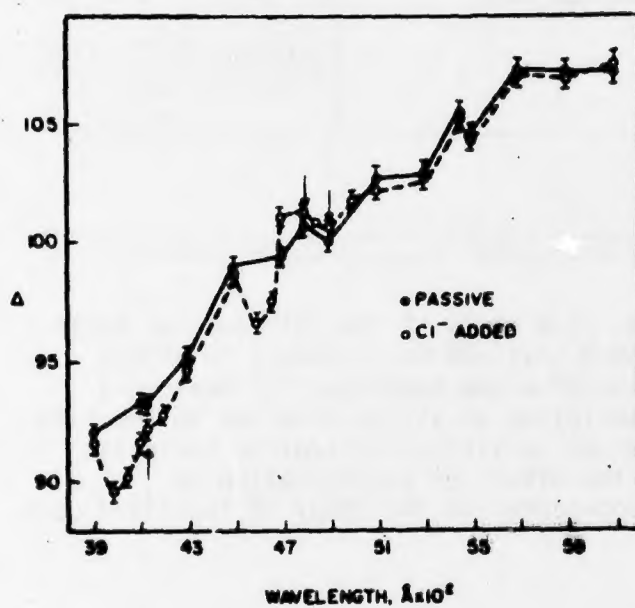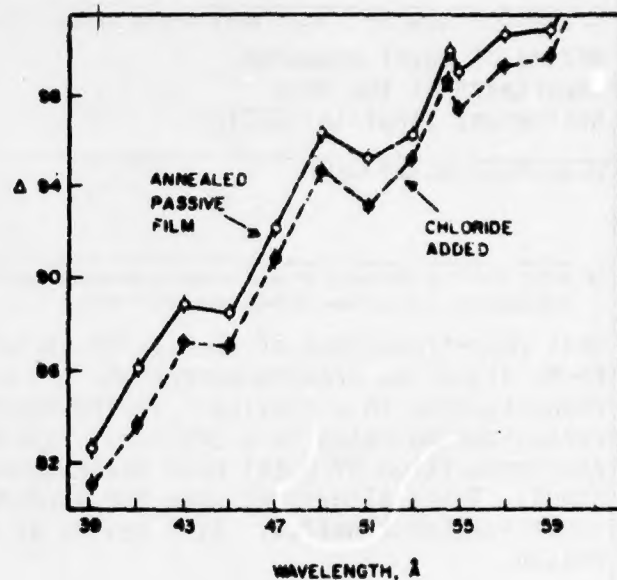   From Ambrose and Kruger (23).

-51-

Fig. 8. A schematic representation of the results obtained in constant
strain-rate tests. Region A—repassivation is rapid enough
and strain rate slow enough to prevent damaging interaction
with the environment. Region B—strain rate high enough so
that repassivation does not prevent environmental access.
Region C—strain rate is so rapid that ductible pulling apart
takes place.

-52-

Fig. 9. A comparison of the effect of the addition of chloride ions on the ellipsometric spectrum (relative phase retardation, Δ, vs. wavelength) obtained for a passive film formed on iron in sodium tetraborate-boric acid solution by polarizing at 1000 mV (SHE) to the spectrum of a similar passive film annealed for 1 hr. at 75°C. a) unannealed film; b) annealed film. From McBee and Kruger (48).

NBS-114A (REV. 7-73)

U.S. DEPT. OF COMM. BIBLIOGRAPHIC DATA SHEET	1. PUBLICATION OR REPORT NO. NBSIR 76-1170	2. Gov't Accession No.	3. Recipient's Accession No.

4. TITLE AND SUBTITLE

The Role of Passive Film Growth Kinetics and Properties in Stress Corrosion and Crevice Corrosion Susceptibility - Technical Report No. 7

5. Publication Date

November 1976

6. Performing Organization Code

7. AUTHOR(S)

J. Kruger and J.R. Ambrose

8. Performing Organ. Report No.

9. PERFORMING ORGANIZATION NAME AND ADDRESS

NATIONAL BUREAU OF STANDARDS
DEPARTMENT OF COMMERCE
WASHINGTON, D.C. 20234

10. Project/Task/Work Unit No.
3120448

11. Contract/Grant No.
NAONR 18-69, NR036-082

12. Sponsoring Organization Name and Complete Address (Street, City, State, ZIP)

Office of Naval Research
Department of the Navy
Arlington, Virginia 22217

13. Type of Report & Period Covered

interim 10/75-11/76

14. Sponsoring Agency Code

15. SUPPLEMENTARY NOTES

16. ABSTRACT *(A 200-word or less factual summary of most significant information. If document includes a significant bibliography or literature survey, mention it here.)*

This report consists of four parts as follows: I-A study of the influence of Mo in Fe-Mo alloys on crevice corrosion. It was found that >5% Mo is needed to affect repassivation in a crevice. II-The description of a new technique for measuring repassivation rates in a crevice. III-A description of alloys prepared to simulate the composition of metal near grain boundaries of sensitized austenitic stainless steel. These alloys are used for studies of the effect of sensitization on repassivation kinetics. IV-A review of new approaches in the study of localized corrosion.

17. KEY WORDS *(six to twelve entries; alphabetical order; capitalize only the first letter of the first key word unless a proper name; separated by semicolons)*

Crevice corrosion; Iron-molybdenum alloys; Localized corrosion; Repassivation; Sensitization; Stainless steel

18. AVAILABILITY	[X] Unlimited	19. SECURITY CLASS (THIS REPORT)	21. NO. OF PAGES
	[ ] For Official Distribution. Do Not Release to NTIS	UNCLASSIFIED	55
	[ ] Order From Sup. of Doc., U.S. Government Printing Office Washington, D.C. 20402, SD Cat. No. C13	20. SECURITY CLASS (THIS PAGE)	22. Price
	[X] Order From National Technical Information Service (NTIS) Springfield, Virginia 22151	UNCLASSIFIED	$ 4.50

USCOMM-DC 29042-P74